Synthesis and spectral analysis of 4-(4-chlorophenyl)-3,4,6,7,8,9-hexahydro-1H-cyclohepta-pyrimidin-2(5H)-one and study of its quantum chemical and thermodynamic properties

Huda Parveen[a], Abha Bishnoi*[a], Shaheen Fatma[b], Poornima Devi[a] & Anil Kumar Verma[a]

[a]Department of Chemistry, University of Lucknow, Lucknow 226 007, India

[b]Department of Chemistry, Shri Ramswaroop Memorial University, Dewa Road, Barabanki 225 003, India

In this article the synthesis and spectral analysis of a novel compound 4 (4-(4-chlorophenyl)-3,4,6,7,8,9-hexahydro-1H-cyclohepta-pyrimidin-2(5H)-one) has been deliberated. The aim of the synthesis is to obtain biologically active pyrimidin-2-one scaffold and to correlate its quantum chemical properties with its experimental results. The structure of the compound has been characterized by using different spectral analysis. The chemical calculations have been computed with the help of DFT level of theory using Becke3–Lee–Yang–Parr (B3LYP))/6-31G(d,p) basis set. DFT computed total first static hyperpolarizability β_{tot} =3.1686 ×10^{-30} esu, indicates that the molecule could be an area of interest as an attractive future NLO material. Electrophilic and nucleophilic regions have been identified with the help of MESP plot. For the analysis of thermal behaviour of compound **4**, thermodynamic properties such as heat capacity, entropy and enthalpy change at various temperatures have been calculated. A close examination of various structural and thermodynamic parameters such as electrostatic potential, electrophilicity (ω), chemical potential (μ), chemical hardness (η) and maximum amount of electronic charge transfer (ΔNmax) have been done for the compound **4**. The local reactivity descriptors show that C(9) is the most reactive site for nucleophilic attack. In addition to it a discussion about correlation graphs between experimental and calculated ^{1}HNMR and ^{13}CNMR spectroscopic values have also been done.

Keywords: Density functional theory (DFT), Natural bond orbital (NBO), Non linear optical (NLO), Molecular electrostatic potential (MESP)

1 Introduction

There are several pyrimidines that have been prepared from the hydrolysis of nucleic acids such as uracil, thymine and cytosine. Exhaustive literature review brings forward a large number of compounds having pyrimidine nucleus, which exhibit a broad range of biological activities like 5-flourouracil possesses anticancer activity, idoxuridine and triflouridine show antiviral activity, zidovudine and stavudine possess anti-HIV activity, trimethoprim, sulphamethiazine and sulphadiazine exhibit antibacterial activity, minoxidil and prazosin serve as antihypertensive drugs, phenobarbitone is used as sedative, hypnotic and anticonvulsant. Propylthiouracil and thinozylamine show antithyroid and H$_1$-antihistaminic activities, respectively, fervennuline shows antibiotic, anticancer, and antitumor activities[1-8]. Now a day's multi-component reactions (MCRs) are drawing the attention of chemists as these reactions have considerable importance in organic and medicinal chemistry[9-12]. Biginelli reactions are one of the most facile tools for the synthesis of complex heterocyclic scaffolds having therapeutic and pharmacological properties[13-15]. In the present paper the synthesis, characterization and a complete description of the molecular geometry, vibrations and electronic features of compound 4 have been discussed. From the literature survey it had been found that such type of compounds were synthesized by multi-component biginelli condensation of cycloalkanones (except cycloheptanone), urea or thiourea and aldehydes[16]. To the best of our knowledge, neither the synthesis, nor the quantum chemical calculations of compound **4** have been illustrated yet. The DFT calculations including NLO, NBO, MESP, electronic absorption spectra, Mulliken atomic charges, global reactivity descriptors and thermodynamic properties have been investigated using density functional theory (DFT) method with B3LYP function using 6-31G (d,p) basis atomic set. The non bonding orbital properties of the compound **4** provide information about distribution of density of electrons in various bonding and anti-
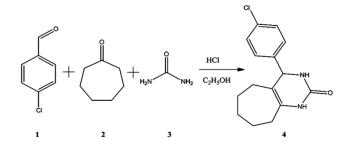
bonding orbitals. Global reactivity descriptors like ionization potential, electron affinity, electronegativity, electrophilicity index and chemical potential have been computed to predict the reactivity of the molecule. The compound has positive aspects for further studies of nonlinear optical properties.

2 Materials and Method

All chemicals were purchased from Alfa Aesar and Sigma–Aldrich. Perkin–Elmer FTIR spectrophotometer and Bruker 300 MHz instrument were used for recording infrared (IR) and ^{1}H and ^{13}C NMR spectra, respectively. The DART-MS of compound was recorded on a JEOL AccuTOF JMS-T100LC mass spectrometer having a DART source. UV spectrum was recorded on UV–visible double-beam spectrophotometer (systronic-2203) instrument. $CDCl_3$ was used as solvent. Melting point was determined in a melting point apparatus and was uncorrected.

2.1 General procedure for synthesis of 4-(4-chlorophenyl)-3,4,6,7,8,9-hexahydro-1H-cyclohepta-pyrimidin-2(5H)-one [(compound 4)]

The product **4** was synthesized by known classical biginelli reaction[16]. The synthetic route for compound **4** was illustrated in Scheme 1. A mixture of 0.006 mol of the 4-chlorobenzaldehyde(1), 0.01 mol of cycloheptanone(2), 0.015 mol of urea(3) and 4-5 drops of conc. HCl in 10 mL of ethanol was refluxed for 8-10 h. The completion of reaction was monitored on TLC and was left overnight. The solid thus formed was collected, washed with luke warm water, dried and recrystallized with ethanol. Yield: ~46%; m.p.: 220 ℃; Rf value: 0.704 using Hexane:Ethyl Acetate (3:7 v/v); IR (KBr) v_{max}: 3423.80 (Asymmetric N-H stretching); 3242.48 (C-H stretching, aromatic); 3091.06(C-H stretching, aliphatic); 1696.47 (C=O stretching); ^{1}HNMR (in $CDCl_3$): δ: 1.17-2.309 (m, 10H), 6.7 (s, NH), 9.91 (s, NH), 7.436-7.775(m, 4H),

7.436 (s, 1H); ^{13}CNMR(in $CDCl_3$): δ: 25.58, 27.82, 30.04, 31.42, 43.57, 128.83, 130.83, 134.18, 134.46, 134.59, 141.43,204.85. MS, m/z: 277.1099.

3 Computational Methods

In this study, Gaussian 09 program package has been used for the calculations. The analysis of results has been done with the help of gauss view 5.0 molecular visualization program[17-20]. The hybrid functional B3LYP[21, 22] and basis set 6-31G(d,p) of DFT[23-25] have been applied to calculate the optimized geometrical parameters and vibrational frequencies of compound **4**. In the NBO basis, the donor–acceptor interactions have been obtained by applying the second-order fock matrix[26]. TD-DFT method has been put forth for calculating UV–Vis spectra, electronic transitions and electronic properties such as HOMO–LUMO energies.

4 Results and Discussion

4.1 Molecular geometry

Table 1 shows the relevant structural parameters of compound **4** which have been obtained by DFT technique. No symmetry constraint has been noticed during geometry optimization. Figure 1 gives the information about the different atoms in the molecule. As all the experimental data is not available for the compound **4**, some of the structural parameters of some other compounds which have similar systems for which the crystal structures have been solved, were used for comparison[27,28]. The optimized structure and experimental structure showed that there was quite less deviation between the geometry optimization and the experimental conformation. The point group symmetry of the compound **4** is C1. The N8-H30 bond distance is shorter than the N10-H31 bond distance. Calculations showed larger bond angle between C3-C4-C5 of compound **4**.

4.2 ^{1}HNMR and ^{13}CNMR spectroscopy

^{1}H and ^{13}C NMR chemical shifts have been computed with GIAO approach using B3LYP/6-31G(d,p) basis set[29,30]. Table 2 shows the experimental and calculated values of ^{1}H and ^{13}C NMR chemical shifts of compound **4**. Chemical shift of any 'X' proton has been calculated by the following expression:

CSX=IMSTMS–IMSX

where CSX-chemical shift of 'X' proton, IMSTMS-isotropic magnetic shielding of TMS and IMSX-

Scheme 1 – Synthesis of 4-(4-chlorophenyl)-3,4,6,7,8,9-hexahydro-1H-cyclohepta-pyrimidin-2(5H)-one (4).

Table 1 – Experimental and calculated optimized geometrical parameters of compound **4** using B3LYP/6-31G(d,p) method.

Bond length	B3LYP	EXP (a,b)	Bond angle	B3LYP	EXP (a,b)	Bond angle	B3LYP	EXP[30] (a,b)
C1-C2	1.54	1.528	C2-C1-C7	114.53	113.5	C9-N8-H30	113.80	115
C1-C7	1.54	1.528	C2-C1-H20	109.51		N8-C9-N10	113.99	114
C1-H20	1.09	1.11	C2-C1-H21	109.17		N8-C9-O12	122.28	123.7
C1-H21	1.09	1.11	C7-C1-H20	107.43		N10-C9-O12	123.70	122.3
C2-C3	1.53	1.528	C7-C1-H21	109.66		C9-N10-C11	126.23	126.7
C2-H22	1.09	1.11	H20-C1-H21	106.18		C9-N10-H31	112.93	
C2-H23	1.09	1.11	C1-C2-C3	113.79	113.5	C11-N10-H31	117.77	
C3-C4	1.54	1.528	C1-C2-H22	108.80		C6-C11-N10	110.82	
C3-H24	1.09	1.11	C1-C2-H23	109.83		C6-C11-C13	112.51	
C3-H25	1.09	1.11	C3-C2-H22	109.79		C6-C11-H32	107.67	
C4-C5	1.51	1.528	C3-C2-H23	108.43		N10-C11-C13	111.84	
C4-H26	1.10	1.11	H22-C2-H23	105.86		N10-C11-H32	107.17	
C4-H27	1.10	1.11	C2-C3-C4	113.18	113.5	C13-C11-H32	106.46	
C5-C6	1.34		C2-C3-H24	110.32		C11-C13-C14	120.62	
C5-N8	1.40		C2-C3-H25	109.73		C11-C13-C18	120.81	
C6-C7	1.51	1.528	C4-C3-H24	110.73		C14-C13-C18	118.55	
C6-C11	1.52		C4-C3-H25	106.90		C13-C14-C15	121.30	
C7-H28	1.09	1.11	H24-C3-H25	105.61		C13-C14-H33	119.62	
C7-H29	1.09	1.11	C3-C4-C5	118.47	113.5	C15-C14-H33	119.07	
N8-C9	1.38	1.371	C3-C4-H26	109.86		C14-C15-C16	118.87	
N8-H30	1.01	0.86	C3-C4-H27	107.52		C14-C15-H34	120.90	
C9-N10	1.37	1.376	C5-C4-H26	108.61		C16-C15-H34	120.22	
C9-O12	1.22	1.215	C5-C4-H27	106.17		C15-C16-C17	121.08	
N10-C11	1.46	1.371	H26-C4-H27	105.34		C15-C16-Cl19	119.52	
N10-H31	1.01	0.88	C4-C5-C6	127.97		C17-C16-Cl19	119.38	
C11-C13	1.53		C4-C5-N8	111.89		C16-C17-C18	119.15	
C11-H32	1.10		C6-C5-N8	120.12		C16-C17-H35	119.99	
C13-C14	1.39	1.395	C5-C6-C7	124.08		C18-C17-H35	120.84	
C13-C18	1.40	1.39	C5-C6-C11	120.08		C13-C18-C17	121.02	
C14-C15	1.39	1.382	C7-C6-C11	115.78		C13-C18-H36	119.64	
C14-H33	1.08		C1-C7-C6	115.53	113.5	C17-C18-H36	119.33	
C15-C16	1.39	1.39	C1-C7-H28	109.13				
C15-H34	1.08		C1-C7-H29	108.36				
C16-C17	1.39	1.381	C6-C7-H28	109.88				
C16-Cl19	1.75	1.737	C6-C7-H29	108.69				
C17-C18	1.39	1.385	H28-C7-H29	104.66				
C17-H35	1.08		C5-N8-C9	124.49	122.7			
C18-H36	1.08		C5-N8-H30	119.78	122			

Dihedral angle

	B3LYP		B3LYP		B3LYP
C7-C1-C2-C3	28.86	C3-C4-C5-C6	13.64	C9-N10-C11-C6	-23.548
C7-C1-C2-H22	151.63	C3-C4-C5-N8	-166.8	C9-N10-C11-C13	102.89
C7-C1-C2-H23	-92.90	H26-C4-C5-C6	-112.5	C9-N10-C11-H32	-140.77
H20-C1-C2-C3	-91.87	H26-C4-C5-N8	66.957	H31-N10-C11-C6	177.73
H20-C1-C2-H22	30.89	H27-C4-C5-C6	134.58	H31-N10-C11-C13	-55.83
H20-C1-C2-H23	146.36	H27-C4-C5-N8	-45.90	H31-N10-C11-H32	60.49
H21-C1-C2-C3	152.26	C4-C5-C6-C7	2.02	C6-C11-C13-C14	-121.45
H21-C1-C2-H22	-84.97	C4-C5-C6-C11	179.46	C6-C11-C13-C18	59.38
H21-C1-C2-H23	30.49	N8-C5-C6-C7	-177.45	N10-C11-C13-C14	113.03
C2-C1-C7-C6	51.74	N8-C5-C6-C11	-0.013	N10-C11-C13-C18	-66.12
C2-C1-C7-H28	-72.63	C4-C5-N8-C9	167.78	H32-C11-C13-C14	-3.72
C2-C1-C7-H29	173.93	C4-C5-N8-H30	4.53	H32-C11-C13-C18	177.11
H20-C1-C7-C6	173.62	C6-C5-N8-C9	-12.65	C11-C13-C14-C15	-179.37
H20-C1-C7-H28	49.24	C6-C5-N8-H30	-175.90	C11-C13-C14-H33	0.580
H20-C1-C7-H29	-64.18	C5-C6-C7-C1	-63.79	C18-C13-C14-C15	-0.19

(*Contd.*)

Table 1 – Experimental and calculated optimized geometrical parameters of compound **4** using B3LYP/6-31G(d,p) method. (*Contd.*)

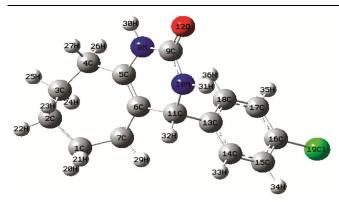|	B3LYP		B3LYP		B3LYP
H21-C1-C7-C6	-71.39	C5-C6-C7-H28	60.19	C18-C13-C14-H33	179.75
H21-C1-C7-H28	164.22	C5-C6-C7-H29	174.18	C11-C13-C18-C17	179.15
H21-C1-C7-H29	50.80	C11-C6-C7-C1	118.66	C11-C13-C18-H36	-0.86
C1-C2-C3-C4	-85.08	C11-C6-C7-H28	-117.34	C14-C13-C18-C17	-0.02
C1-C2-C3-H24	39.61	C11-C6-C7-H29	-3.354	C14-C13-C18-H36	179.96
C1-C2-C3-H25	155.58	C5-C6-C11-N10	15.77	C13-C14-C15-C16	0.22
H22-C2-C3-C4	152.68	C5-C6-C11-C13	-110.29	C13-C14-C15-H34	-179.88
H22-C2-C3-H24	-82.60	C5-C6-C11-H32	132.69	H33-C14-C15-C16	-179.72
H22-C2-C3-H25	33.36	C7-C6-C11-N10	-166.57	H33-C14-C15-H34	0.158
H23-C2-C3-C4	37.45	C7-C6-C11-C13	67.35	C14-C15-C16-C17	-0.038
H23-C2-C3-H24	162.15	C7-C6-C11-H32	-49.65	C14-C15-C16-Cl19	179.98
H23-C2-C3-H25	-81.87	C5-N8-C9-N10	6.29	H34-C15-C16-C17	-179.92
C2-C3-C4-C5	44.88	C5-N8-C9-O12	-172.32	H34-C15-C16-Cl19	0.098
C2-C3-C4-H26	170.48	H30-N8-C9-N10	170.43	C15-C16-C17-C18	-0.17
C2-C3-C4-H27	-75.36	H30-N8-C9-O12	-8.18	C15-C16-C17-H35	179.91
H24-C3-C4-C5	-79.60	N8-C9-N10-C11	13.25	Cl19-C16-C17-C18	179.80
H24-C3-C4-H26	45.99	N8-C9-N10-H31	172.85	Cl19-C16-C17-H35	-0.104
H24-C3-C4-H27	160.15	O12-C9-N10-C11	-168.15	C16-C17-C18-C13	0.204
H25-C3-C4-C5	165.81	O12-C9-N10-H31	-8.54	C16-C17-C18-H36	-179.77
H25-C3-C4-H26	-68.58	H35-C17-C18-H36	0.12	H35-C17-C18-C13	-179.88
H25-C3-C4-H27	45.57				

Fig. 1 – Optimized geometry of compound 4 using B3LYP/6-31G(d,p) level of theory.

isotropic magnetic shielding of 'X' proton. For ^{1}HNMR the correlation graph follows the linear equation y =1.102x – 0.236 and for ^{13}CNMR it follows the linear equation y = 1.244x – 7.549 using B3LYP, where y and x are experimental and calculated chemical shifts, respectively. Experimental ^{1}H and ^{13}CNMR spectra show good agreement with calculated ^{1}H and ^{13}C NMR spectra except H30 and H31 (Fig. 2 and Fig. 3).

4.3 UV–Visible absorption spectroscopy

Integral equation formalism polarizable continuum model (IEFPCM) has been implemented to find out the solvent effect. The UV data obtained through DFT and related properties have been ordered in Table 3 and compared with experimental UV data. One intense electronic transition at 220.45 nM with an

oscillator strength f = 0.6297 in DMSO (dimethyl sulfoxide) is obtained which is in good concord with the experimental data (λexp. = 218 nM in DMSO) (Fig. 4). This absorption be in tuned with the transition from the HOMO(73) to the LUMO+3(77) with 39.65% contribution. Calculated UV spectrum of title molecule shows a band around 186.95 nM (in DMSO) which is electronic transition from HOMO-4(69) to LUMO+1(75) with 22.13% contribution. In the compound **4** these transitions appeared to be due to σ→σ* transition. Molecular orbitals of the compound and their electronic transitions have been shown in Fig. 5.

HOMO is mainly localized on the pyrimidine ring, slightly delocalized on carbon atoms of aromatic ring attached to Cl atom and on two neighboring carbon and hydrogen atoms of cycloheptene ring. LUMO is delocalized over the aromatic ring, nitrogen atom nearest to the aromatic ring and carbonyl function (C=O) of pyrimidine ring. LUMO+1 is localized on aromatic ring but slightly delocalized over pyrimidine ring and HUMO-4 is delocalized over both cycloheptene and pyrimidine rings. The value of the energy gap between HOMO and LUMO+3 is 5.6241 eV. This manifests the chemical reactivity of the compound **4** and the existance of terminal charge transfer inside the molecule.

4.4 Vibrational assignments

Table 4 shows the observed and calculated infrared wave numbers and vibrations. A slightly higher

Table 2 – Experimental and calculated ^{1}H and ^{13}C NMR of compound **4** using B3LYP functional and 631-G/(d,p) basis set.

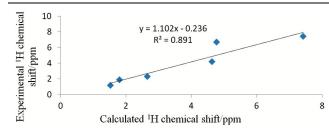| Atoms	Calculated ^{13}CNMR BL3YP (ppm)	Experimental (ppm)	Assignment	Atoms	Calculated ^{1}HNMR BL3YP (ppm)	Experimental (ppm)	Assignment
C1	31.29		Cycloheptene carbons	H20	1.52		6 protons of cycloheptene ring
C2	28.29	25.58-43.57		H21	1.84	1.173	
C3	25.75			H22	1.73		
C4	38.75			H23	1.7		
C7	29.28			H24	1.92		
C5	131.63	141.43	C=C carbons of pyrimidine ring	H25	1.53		
C6	107.5	134.59		H26	2.65		4 protons of cycloheptene ring bonded to the carbon adjacent to C=C.
C9	145.51	204.85	C=O carbon	H27	2		
C13	143.67		Aromatic carbons	H28	2.43	1.886-2.309	
C14	127.16	128.83-134.46		H29	1.2		
C15	126.17			H30	4.77	9.91	2 protons of two (–NH-) group
C16	140.05			H31	3.79	6.7	
C17	127.82			H32	4.63	7.436	1 methyne proton
C18	127.78			H33	7.18		4 prot-ons of aromatic ring
				H34	7.25		
				H35	7.42		
				H36	7.78	7.436-7.775	

Fig. 2 – Correlation graph between calculated and experimental ^{1}H NMR chemical shifts.
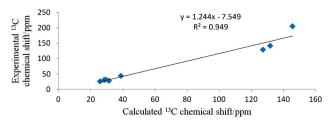

Fig. 3 – Correlation graph between calculated and experimental ^{13}CNMR chemical shifts.

vibrational wavenumbers have been obtained because of the presence of discarded anharmonicity in the real system. Therefore, calculated wavenumbers have been scaled down by a single factor[23] 0.9679 compared with experimental wavenumbers. The value of correlation coefficient (R^2 =0.994) showed that there is good agreement between experimental and calculated wavenumbers (Fig. 6). The experimental and theoretical IR spectra using B3LYP/6-31G(d,p) have been shown in Fig. 7.

4.5 Molecular electrostatic potential

The reactive sites of the compound **4** for electrophilic and nucleophilic attack can be predicted with the help of molecular electrostatic potential map (MESP). The molecular size, shape and electrostatic potential of the molecule can be detected with the help of MESP surface in terms of color grading and the correlation between molecular structure and the physiochemical properties relationship of molecule can also be detected by this MESP surface[31-33]. The electron rich and electron poor regions are referred by the red and blue regions respectively while green region in the MESP suggests the almost neutral region. It has been observed that the molecule produces the variation in electrostatic potential that is largely responsible for the binding of a drug to its receptor binding sites, as the binding sites in general are expected to have opposite areas of electrostatic potential. Gauss view software has been used to generate the MESP map of the compound **4** (Fig. 8). MESP of compound **4** clearly shows that there is major negative potential region around oxygen atom, characterized by red color and electrophilic attack occurs at this site. The H atoms of amino group bear the maximum brunt of positive potential while rest of the molecule seems to have almost neutral electrostatic potential.

4.6 Natural bond orbital analysis

The natural bond orbital (NBO) calculations[34] have been performed using Gaussian03 package at the

Table 3 – Experimental and theoretical absorption wavelength λ_{max} (nM), excitation energies E (eV) of compound **4** using B3LYP functional and 631-G/(d,p) basis set.

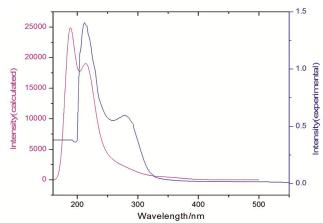| S. No	Electronic transitions(Molecular orbital involved)	Energy (in eV)	Calculated λ_{max} (in nM) B3LYP	Oscillatory strength (f)	Percentage contribution of probable transition B3LYP	Observed λ_{max} (in nM)
1	H→L+3	5.6241	220.45	0.2311	39.65%	218
2	H-4→L+1	6.6328	186.93	0.1741	22.13%	

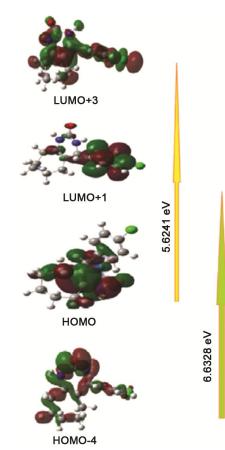Fig. 4 – Experimental and calculated UV–visible spectra of the compound **4**.

Fig. 5 – Molecular orbitals (HOMO→ LUMO+3 and HOMO-4→ LUMO+1) of the compound **4** at the B3LYP/6-31G(d,p) basis set.

B3LYP/6-31G(d,p) method. NBO analysis provides very useful information about the charge transfer or conjugative interactions in molecular systems and intra-molecular and inter-molecular bondings. The interactions among bonds can also be detected by these NBO calculations. The larger the stabilization energy value, the more intensive is the interaction between electron donors and electron acceptors, i.e., the more donating tendency from electron donors to electron acceptors and the greater the extent of conjugation of the whole system. The chemical interpretation of hyperconjugative interaction and electron density transfer from the filled lone pair electron can be obtained by implication of NBO analysis. Interaction between both filled and virtual orbital spaces has been correctly explained by the NBO analysis and it could enhance the analysis of intra-molecular and intermolecular interactions. The interaction between donor level bonds and acceptor level bonds in the NBO analysis has been done by carrying out the second order fock matrix[35]. The result of interaction is a loss of occupancy from the concentration of electron NBO of the idealized Lewis structure into an empty non-Lewis orbital. For each donor (i) and acceptor (j) the stabilization energy E(2) associated with the delocalization i→j is as follows:

$$E(2) = \Delta E_{ij} = qi \frac{\left(F_{ij}\right)^2}{\left(E_j - E_i\right)} \qquad \text{... (1)}$$

where qi →donor orbital occupancy, Ei and Ej → the diagonal elements and Fij →off diagonal NBO Fock matrix element. In NBO analysis the extent of conjugation of the whole system depends on E(2) value, i.e., as the value of E(2) increases the extent of conjugation also increases. The larger values of E(2) shows the intensive interaction between electron-donors and electron-acceptors. The possible intensive interactions (Type1→Type2) causing increased electron density (ED) and intra-molecular charge transfer (ICT) leading to the stabilization of the system have been given in NBO Table 5. The elongation and red shift both have been explained by

Table 4 – Experimental and calculated vibrational frequencies (cm^{-1}) of compound **4**.

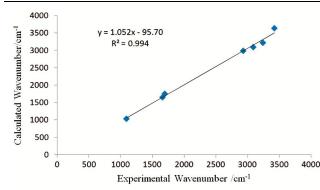| Experimental	Calculated (B3LYP)	Vibrational assignment	Characteristic Absorptions (cm^{-1})
3423.8	3637.28	Asymmetric N-H stretching	The N-H stretching vibrations are obtained between 3500-3140cm^{-1}.
3242.48	3219.40	Aromatic =C-H stretching	The aromatic C-H stretching vibrations are normally found between 3100 and 3000 cm^{-1} due to aromatic C-H stretching vibrations [32]. In the (compound 4) the aromatic ring is attached to another 6 member ring which in turn further fussed with a 7 member ring therefore aromatic C-H stretching vibrations appeared at lower frequency
3091.06	3091.85	Aliphatic -C-H stretching	Aliphatic -C-H stretching vibrations are obtained between 2850-3000cm^{-1}.
2932.81	2987.15	Aromatic C-H stretching	The aromatic C-H stretching vibrations are normally found between 3100 and 3000 cm^{-1}
1696.47	1750.14	C=O stretching	Amide shows lower carbonyl stretching frequency, absorbing around 1650-1690 cm^{-1}. In conjugated amides the carbonyl stretching frequency is lowered.
1661.75	1648.36	N-H in plane bending	The N-H bending vibrations are obtained between1550-1640cm^{-1}.
1092.72	1028.95	C-N stretching	The C-N stretching vibrations are obtained between 1030- 1230cm^{-1}.

Fig. 6 – Correlation graph between calculated and experimental wavenumbers.

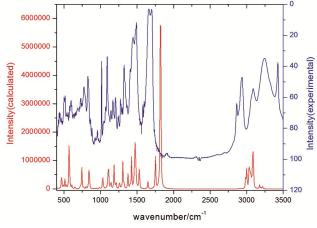Fig. 8 – The molecular electrostatic potential of compound **4**.

Fig. 7 – Experimental and theoretical [using B3LYP/6-31G(d,p)] IR spectra of compound **4**.

the electron density which is transferred from σ*(C15-C16), n(O) and n(N) to antibonding σ* and π* orbital of C-N, C-C and C-O.

4.7 Non linear optical analysis

The key functions of frequency shifting, optical switching, optical modulation, optical logic and optic
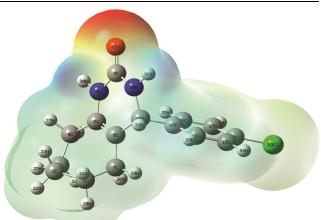
memory for the emerging technologies in areas such as telecommunications, signal processing and optical interconnections[36-38] can be obtained from the NLO studies of the molecules. The study of NLO effect has great importance in the current research. Nonlinear optics gives information about the interaction of applied electromagnetic fields in diverse compounds to generate new electromagnetic fields, altered in wavenumber, phase or other physical properties. Technologically important organic molecules are those which can manipulate photonic signals efficiently. The B3LYP/6-31G(d,p) basis set based on the finite field approach has been used to calculate first hyperpolarizability of the compound **4**. In the presence of an applied electric field, the energy of a system is a function of electric field. The first hyperpolarizability is a third rank tensor and 3x3x3 matrix has been used to describe it. The 27 components of the matrix can be reduced to 10 components due to Kleinman symmetry[39]. Following

Table 5 – Second order perturbation theory analysis of fock matrix in NBO basis of the compound **4**.

Donor (i)	Type1	ED/e	Acceptor(j)	Type2	ED/e	$E(2)^a$	$E(j)-E(i)^b$	$F(i,j)^c$	Type1→Type2
C13-C14	σ	1.66	C15-C16	σ *	0.38	21.65	0.27	0.069	(C13-C14)σ→σ*(C15-C16)
C13-C14	σ	1.66	C17-C18	σ *	0.30	19.60	0.28	0.067	(C13-C14)σ→σ*(C17-C18)
C15-C16	σ	1.68	C13-C14	σ *	0.34	18.00	0.30	0.066	(C15-C16)σ→σ*(C13-14)
C15-C16	σ	1.68	C17-C18	σ *	0.30	18.74	0.30	0.067	(C15-C16)σ→σ*(C17-18)
C17-C18	σ	1.67	C13-C14	σ *	0.34	19.76	0.29	0.067	(C17-C18)σ→σ*(C13-14)
C17-C18	σ	1.67	C15-C16	σ *	0.38	20.70	0.27	0.067	(C17-C18)σ→σ*(C15-16)
C15-C16	σ	0.38	C13-C14	σ *	0.34	168.9	0.02	0.083	(C15-C16)σ→σ*(C13-C14)
C15-C16	σ	0.38	C17-C18	σ *	0.30	164.7	0.02	0.079	(C15-C16)σ→σ*(C17-C18)
LP(1)N8	n	1.72	C5-C6	π*	0.18	33.69	0.32	0.095	[LP(1)N8] n→π*(C5-C6)
LP(1)N8	n	1.72	C9-O12	π*	0.33	39.05	0.35	0.106	[LP(1)N8]n→π*(C9-O12)
LP(1)N10	n	1.75	C9-O12	π*	0.33	40.35	0.35	0.108	[LP(1)N10]n→π*(C9-12)
LP(2)O12	n	1.85	N8-C9	σ *	0.08	26.07	0.67	0.120	[LP(2)O12]n→σ *(N8-C9)
LP(2)O12	n	1.85	C9-N10	σ *	0.075	25.15	0.70	0.120	[LP(2)O12]n→σ*(C9-N10)

$E(2)^a$ – energy of hyperconjugative interaction (stabilization energy in Kcal/mol);
$E(j)-E(i)^b$ – Energy difference between donor and acceptor i and j NBO orbitals in a.u;
$F(i,j)^c$ – is the fock matrix elements between i and j NBO orbital in a.u.

equations have been used to calculate the magnitude of total dipole moment μ, the average polarizability α_{tot} and the first hyperpolarizability β_{tot}, using the x, y, z components:

$$\mu_{tot} = \left(\mu_x^2 + \mu_y^2 + \mu_z^2 \right)^{1/2} \qquad \ldots (2)$$

$$\alpha_{tot} = \frac{1}{3}\left(\alpha_{xx} + \alpha_{yy} + \alpha_{zz} \right) \qquad \ldots (3)$$

$$\langle \beta \rangle = \left[\left(\beta_{xxx} + \beta_{xyy} + \beta_{xzz} \right)^2 + \left(\beta_{yyy} + \beta_{yzz} + \beta_{yxx} \right)^2 + \left(\beta_{zzz} + \beta_{zxx} + \beta_{zyy} \right)^2 \right]^{1/2}$$
$$\ldots (4)$$

The results of electronic dipole moment μ_i (i = x, y, z), polarizability α_{ij} and first order hyperpolarizability β_{ijk} have been listed in the Table 6. The calculated dipole moment is equal to 3.880D forB3LYP level. The calculated polarizability α_{tot} is equal to 26.3772×10^{-24}esu for B3LYP level. The calculated first hyperpolarizability of the compound **4** is 3.1686×10^{-30} esu for B3LYP level and this value is greater (24.3738 times for B3LYP level) than that of the standard NLO material urea[40] $(0.13 \times 10^{-30}$ esu). Based on nonlinear optical properties, it has been found that compound **4** is an attractive object for future studies.

4.8 Thermodynamic properties

All the thermodynamic parameters have been recorded by DFT using B3LYP functional with 6-31G(d,p) basis set. The values of some thermodynamic parameters of compound **4** have been shown in the Table 7. All these parameters have been

Table 6 – Dipole moment μ_i, polarizability α_{tot} and first order hyperpolarizability β_{tot} data for compound **4** calculated at DFT/B3LYP/6-31G(d,p) level of theory.

Dipole moment	B3LYP	Hyperpolarizability	B3LYP
μ_x	-2.1946	β_{xxx}	-198.5830
μ_y	-3.1777	β_{xxy}	-36.0401
μ_x	0.4502	β_{xyy}	15.1355
μ_{tot}	3.880	β_{yyy}	-257.036
Polarizability		β_{xxz}	53.9697
α_{xx}	225.876	β_{xyz}	24.3321
α_{xy}	-16.9783	β_{yyz}	48.2314
α_{yy}	156.829	β_{xzz}	-13.5313
α_{xz}	6.7753	β_{yzz}	8.9323
α_{yz}	-14.6648	β_{zzz}	20.1710
α_{zz}	151.246	β_{tot}(esu)	3.1686
α_{tot}(esu)	26.3772		

(For α: 1 a.u. $=0.1482 \times 10^{-24}$ esu; β: 1 a.u. $= .0086393 \times 10^{-30}$ esu).

Table 7 – Calculated thermodynamic parameters of compound **4** at standard temperature 298.15 K.

Parameters	B3LYP6-31G(d,p)
Zero point vibrational energy (Kcal/mol)	187.65958
Rotational temperature(K)	0.02644
	0.00908
	0.00778
Rotational constant(GHZ)	
X	0.55098
Y	0.18915
Z	0.16205
Total energy E_{total}(Kcal/mol)	198.107
Translational	0.889
Rotational	0.889
Vibrational	196.330

obtained at standard temperature 298.15 K. The standard statistical thermodynamic functions, heat capacity (CV) and entropy (S) have been recorded at diverse temperatures (100–500K) for compound **4** on the basis of vibrational analysis and have been listed in Table 8. It has been observed that the molecular vibrational intensities and the standard statistical thermodynamic functions[41,42] increase with temperature ranging from 100 K to 500 K. The correlation equations among heat capacities, entropies and temperatures are fitted by quadratic formulas and the corresponding fitting factors (R^2) for these thermodynamic properties are given in Eqs (5) and (6). The correlation graphics are shown in Fig. 9.

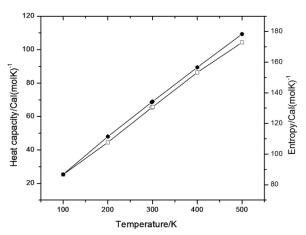$$S = 3.6311 + 0.2138T - 5.10^{-2}T^2 \qquad ...(5)$$
$$[R^2 = 0.999]$$

Fig. 9 – Correlation graphs of heat capacity and entropy calculated at different temperatures using B3LYP.

Table 8 – Thermodynamic functions of compound **4** at different temperatures.

Temperature (K)	Heat capacity(CV) (cal/MolK)(B3LYP)	Entropy(S) (cal/MolK)(B3LYP)
100	25.240	86.780
200	44.550	111.452
298	65.302	133.865
300	65.698	134.282
400	86.378	156.633
500	104.313	178.338

$$CV = 61.85 + 0.2553T - 5.10^{-4}T^2 \qquad ...(6)$$
$$[R^2 = 0.999]$$

Change in Gibbs free energy and the spontaneity of the reaction can be achieved by implementation of these equations.

4.9 Chemical reactivity descriptor
4.9.1 Global reactivity descriptors

Global reactivity descriptors predict global reactivity trends. The energies of frontier molecular orbitals (ƐLUMO, ƐHOMO), band gap (ƐLUMO-ƐHOMO), ionization potential (IP), electron affinity (EA), electronegativity (χ), global hardness(η), chemical potential (μ), global electrophilicity index (ω), global softness (S)[43-47] and additional electronic charge (N_{max}) of reactant **1, 2** and product **4** have been calculated (Table 9).

A global reactivity index is an electrophilicity index (ω). This is a positive and definite quantity. The stabilization in energy has been measured by this new reactivity index when the system gains an additional electronic charge (ΔN) from the environment. Electrophilic charge transfer[48] (ECT) can be obtained by calculating the difference between the ΔN_{max} values of interacting molecules. The calculated value of ECT>0 for reactant molecules. Reactants 4-chlorobenzaldehydes (**1**) and cycloheptanone (**2**) indicates charge flows from reactant **1** to **2**. Therefore, the reactant molecule **1** behaves as global nucleophile (electron donor) and molecule **2** as global electrophile (electron acceptor). The higher value of electrophilicity index ω =1.9578 eV of product **4** than reactant **2** indicates that it is strong electrophile than reactant **2**.

4.9.2 Local reactivity descriptors

Fukui function (f_K) is used to describe the chemical reactivity, site selectivity, the local softness (S_K^+, S_K^-, S_K^0) and electrophilicity indices (ω_K^+, ω_K^-, ω_K^0). The more prone site for nucleophilic or electrophilic attack can be investigated by knowing the values of these three local reactivity descriptors ($S_K^\pm$, $f_K^\pm$, $\omega_K^\pm$). Fukui functions ($f_K^\pm$), local softness

Table 9 – Calculated frontier molecular orbitals (ƐLUMO, ƐHOMO), band gap (ƐLUMO-ƐHOMO), ionization potential (IP), electron affinity (EA), electronegativity (χ), global hardness(η), chemical potential (μ), global electrophilicity index (ω), global softness (S) and additional electronic charge (ΔN_{max}) of reactant **1, 2** and product **4** using B3LYP/6-31G(d,p) basis set.

	ε_H	ε_L	$\varepsilon_H - \varepsilon_L$	IP	EA	χ	η	μ	ω	S	ΔN_{max}
1	-7.152	-1.996	-5.155	7.1521	1.9962	4.5741	2.5779	-4.5741	4.0580	0.1939	1.7743
2	-6.364	-0.268	-6.096	6.3641	0.268	3.3160	3.0480	-3.3160	1.8038	0.1640	1.0879
4	-5.611	-0.632	-4.979	5.6117	0.6327	3.1222	2.4895	-3.1222	1.9578	0.2008	1.2541

Table 10 – Hirshfeld population analysis: Fukui functions (f_k^+, f_k^-), Local softnesses (s_k^+, s_k^-) in eV, local electrophilicity indices (ωk^+, ωk^-) in eV for selected atomic sites of compound **4**.

Atom No.	Hirshfeld atomic charges			Fukui functions		Local softness		Local electrophilicity indices	
	q_N	q_N+1	q_N-1	f_k+(eV)	f_k-(eV)	sk^+(eV)	sk^-(eV)	$\omega k+$(eV)	$\omega k\bullet$(eV)
1 C	-0.1679	-0.18958	0.01955	-0.02162	-0.18752	-0.00557	-0.04832	-0.07914	-0.68645
2 C	-0.1739	-0.19195	0.01535	-0.01802	-0.18928	-0.00464	-0.04878	-0.06596	-0.6929
3 C	-0.183	-0.19874	0.01315	-0.0156	-0.1963	-0.00402	-0.05059	-0.05709	-0.7186
4 C	-0.2371	-0.25798	-0.0261	-0.02079	-0.21106	-0.00536	-0.05439	-0.07611	-0.77263
5 C	0.2362	0.26184	0.30684	0.02562	-0.07062	0.00660	-0.0182	0.09379	-0.25853
6 C	0.0494	0.12291	0.02700	0.07346	0.02244	0.01893	0.00578	0.26893	0.08215
7 C	-0.2268	-0.2473	-0.0348	-0.02049	-0.19201	-0.00528	-0.04948	-0.07502	-0.70289
8 N	-0.6199	-0.51229	-0.3577	0.10765	-0.26225	0.02775	-0.06758	0.39408	-0.96001
9 C	0.6551	0.67472	0.72427	0.01954	-0.06909	0.00503	-0.01781	0.07154	-0.25293
10 N	-0.5979	-0.53531	-0.2800	0.06266	-0.31795	0.01615	-0.08194	0.22937	-1.16393
11 C	0.0102	-0.03479	0.05856	-0.04501	-0.04835	-0.0116	-0.01246	-0.16478	-0.17698
12 O	-0.4026	-0.31851	-0.5306	0.08411	0.12803	0.02168	0.03299	0.30791	0.46871
13 C	0.0635	0.05625	0.14673	-0.00733	-0.08316	-0.00189	-0.02143	-0.02683	-0.30441
14 C	-0.1142	-0.11549	-0.0447	-0.0013	-0.06946	-0.00033	-0.0179	-0.00475	-0.25429
15 C	-0.0809	-0.07358	0.04235	0.00735	-0.12329	0.00189	-0.03177	0.02693	-0.45134
16 C	-0.0917	-0.08867	-0.0955	0.00303	0.00379	0.00078	0.00097	0.01112	0.01388
17 C	-0.0817	-0.07338	0.04157	0.008363	-0.12332	0.002156	-0.03178	0.030614	-0.45142
18 C	-0.0905	-0.10059	-0.0031	-0.01006	-0.08738	-0.00259	-0.02252	-0.03681	-0.31985
19 Cl	-0.0081	0.065228	-0.0227	0.073351	0.014588	0.018908	0.003759	0.268516	0.053402

($S_\kappa^\pm$) and local electrophilicity indices ($\omega_K^\pm$)[46, 47] for selected atomic sites of molecule have been listed in Table 10.

From Table 10 it can be observed that C5, C6, N8 and N10 sites are more prone to nucleophilic attack because of the relative high value of local reactivity descriptors (S_κ^+, f_κ^+, ω_K^+) whereas O12 and C16 sites are more prone to electrophilic attack because of the relative high value of local reactivity descriptors (S_κ^-, f_κ^-, ω_K^-). Thus new heterocyclic compounds may be synthesized by using this molecule as an intermediate.

5 Conclusions

4-(4-chlorophenyl)-3,4,6,7,8,9-hexahydro-1H-cyclohepta-pyrimidin-2(5H)-one has been synthesized and identified by UV–visible, FT-IR, ^{1}H and ^{13}C NMR spectroscopic methods. It has been accomplished that the lowest singlet excited state of compound **4** is derived from the HOMO → LUMO ($\sigma \to \sigma$ *) electron transition. NBO results reflects the charge transfer within the molecule. The first hyper polarizability of the compound **4** obtained is 3.1686x10^{-30}, which is greater (24.374 times for B3LYP level) than that of the standard NLO material urea (0.13×10^{-30} esu). This has enabled compound 4 to be a potential candidate for nonlinear optical applications. The higher value of electrophilicity

index ω (1.9578 eV) of product **4** than that of reactant **2** indicates that the product **4** is more electrophilic in nature than reactant **2**. The local reactivity descriptors (S_κ^-, f_κ^-, ω_K^-) at O12 and C16 indicate that these sites are more prone to electrophilic attack. The thermodynamical parameters like heat capacity and entropy increase with the increase of the temperature. The NLO analysis including total and partial dipole moment, polarizability and hyperpolarizability values are clearly indicating the fact that the molecule is a good NLO material.

References

1 Gavilan M D, Gomez-Vidal J A & Serrano F R, *Bio Med Chem Lett*, 18 (2008) 1457.
2 Ahmed O M & Mohamad M A, *Eur Med Chem*, 44 (2009) 3519.
3 Mohamed N R, El-Saidi M M T, Alia Y M & Elnagdi M H, *Bioorg Med Chem*, 15 (2007) 6227.

4   Amr A G E, Mohamed A M, Mohamed S F, Hafez N A A &
    Hammam A G, *Bioorg Med Chem*, 14 (2006) 5481.
5   Gangjee A, Kurup S, Ihnat M A, Thorpe J E & Shenoy S S,
    Bioorg Med Chem, 18 (2010) 3575.
6   Ajam M A, Kumar B P R & Suresh B, *Ind J Pharm Sci*,
    (2008) 672.
7   Amin K M, El-Zahar M I, Anwar M M, Kamel M M &
    Mohamed M H, *Acta Poloniae Pharmaceut Drug Res*,
    66 (2009) 279.
8   Kraljevic T G, Kristafor S, Suman L, Kralj M, Ametamey S
    M, Cetina M & Malic S R, *Bioorg Med Chem*, 18 (2010)
    2704.
9   Kappe C O, *Acc Chem Res,* 33 (2000) 879.
10 Armstrong R W, Combs A P, Tempest P A, Brown S D &
    Keating T A, *Acc Chem Res*, 29 (1996) 123.
11 Domling A & Ugi I, *Angew Chem Int Ed*, 39 (2000) 3168.
12 Simon C, Constantieux T & Rodriguez J, *Eur J Org Chem*
    2004 (2004) 4957.
13 Kappe C O, *Tetrahedron*, 49 (1993) 6937.
14 Rovnyak G C, Kimball S D, B Beyer, Cucinotta G, Dimarco
    J D, Gougoutas J, Hedberg A, Malley M, Mccarthy J P,
    Zhang R & Moreland S, *J Med Chem*, 38 (1995) 119.
15 Atwal K S, Rovnyak G C, Kimball S D, Floyd D M,
    Moreland S, Swanson B N, Gougoutas J Z, Schwartz J,
    Smillie K M & Malley M F, *J Med Chem*, 33 (1990) 2629.
16 Zhu Y, Huang S & Pan Y, *Eur J Org Chem*, (2005) 2354.
17 Frisch M J, Trucks G W, Schlegel H B, Scuseria G E,
    Robb M A, Cheeseman J R, MontgomeryJr J A, Vreven T,
    Kudin K N, Burant J C, Millam J M, Iyengar S S, Tomasi J,
    Barone V, Mennucci B, Cossi M, Scalmani G, Rega N,
    Petersson G A, Nakatsuji H, Hada M, Ehara M, Toyota K,
    Fukuda R, Hasegawa J, Ishida M, Nakajima T, Honda Y,
    Kitao O, Nakai H, Klene M, Li X, Knox J E, Hratchian H P,
    Cross J B, Bakken V, Adamo C, Jaramillo J, Gomperts R,
    Stratmann R E, Yazyev O, Austin A J, Cammi R, Pomelli C,
    Ochterski J W, Ayala P Y, Voth K, Morokuma G A,
    Salvador P, Dannenberg J J, Zakrzewski V G, Dapprich S,
    Daniels A D, Strain M C, Farkas O, Malick D K, Rabuck A
    D, Raghavachari K, Foresman J B, Ortiz J V, Cui Q,
    Baboul A G, Clifford S, Cioslowski J, Stefanov B B, Liu G,
    Liashenko A, Piskorz P, Komaromi I, Martin R L, Fox D J,
    Keith T, Al-Laham M A, Peng C Y, Nanayakkara A,
    Challacombe M, Gill P M W, Johnson B, Chen W, Wong M W,
    Gonzalez C, Pople J A, Gaussian 03, Revision C-02,
    Gaussian Inc, Wallingford, CT, (2004).
18 Frisch M J, Trucks G W, Schlegel H B, Scuseria G E, Robb
    M A, Cheeseman J R, Scalmani G, Barone V, Mennucci B,
    Petersson G A, Nakatsuji H, Caricato M, Li X, Hratchian H P,
    Izmaylov A F, Bloino J, Zheng G, Sonnenberg J L, Hada M,
    Ehara M, Toyota K, Fukuda R, Hasegawa J, Ishida M,
    Nakajima T, Honda Y, KitÅ O, Nakai H, Vreven T,
    Montgomery Jr J A, Peralta J E, Ogliaro F, Bearpark M,
    Heyd J J, Brothers E, Kudin K N, Staroverov V N,
    Kobayashi R, Normand J, Raghavachari K, Rendell A,
    Burant J C, Iyengar S S, Tomasi J, Cossi M, Rega N,
    Millam J M, Klene M, Knox J E, Cross J B, Bakken V,
    Adamo C, Jaramillo J, Gomperts R, Stratmann R E, Yazyev O,
    Austin A J, Cammi R, Pomelli C, Ochterski J W, Martin R L,

    Morokuma K, Zakrzewski V G, Voth G A, Salvador P,
    Dannenberg J J, Dapprich S, Daniels A D, Farkas O,
    Foresman J B, Ortiz J V, Cioslowski J & Fox D J, Gaussian 09,
    Revision A1, Gaussian Inc, Wallingford, CT, (2009).
19 Pittsburgh P A, Computer program Gauss View 309, Ver 2,
    Gaussian Inc [SD-008].
20 Frisch E, Hratchian H P, Dennington R D I I, Keith T A,
    Millam J, Nielsen A B, Holder A J & Hiscocks J, Gaussian
    Inc Gauss View Version 508, 2009.
21 Becke A D, *J Chem Phys*, 98 (1993) 5648.
22 Lee C T, Yang W T & Parr R G B, *Phys Rev*, 37 (1988) 785.
23 Karabacak M, *J Mol Struct*, 919 (2009) 215.
24 Petersson D A & Allaham M A, *J Chem Phys*, 94 (1991)
    6081.
25 Petersson G A, Bennett A, Tensfeldt T G, Allaham M A &
    Mantzaris W A J, *J Chem Phys*, 89 (1988) 2193.
26 Sarafran M, Komasa A & Adamska E B, *J Mol Struct*,
    82 (2007) 7101.
27 Dillen J & Geise H J, *J Chem Phys*, 70 (1979) 425.
28 Sampath N, Mathews R & Ponnuswamy M N, *J Chem
    Crystallogr*, 40 (2010) 1110.
29 Wolinski K, Hinton J F & Pulay P, *J Am Chem Soc*,
    112 (1990) 8251.
30 Zhengyu Z, Aiping F & Dongmei D, *J Quantum Chem*,
    78 (2000) 186.
31 Joshi B D, Srivastava A, Honorato S B, Tandon P, Pessao O
    D L, Fechine P B A & Ayala A P, *Spectrochim Acta A*,
    113 (2013) 367.
32 Xavier R J & Dinesh P, *Spectrochim Acta A*, 118 (2014) 999
33 Govindarajan M & Karabacak M, *Spectrochim Acta A*,
    96 (2012) 421.
34 Glendening E D, Reed A E, Carpenter J E & Weinhold F,
    NBO Version 31, TCI, University of Wisconsin, Madison,
    1998.
35 Reed A E, Curtis L A & Weinhold F, *Chem Rev*, 88 (1988)
    899.
36 Andraud C, Brotin T, Garcia C, Pelle F, Goldner P, Bigot B
    & Collet A, *J Am Chem Soc*, 116 (1994) 2094.
37 Nakano M, Fujita H, Takahata M & Yamaguchi K,
    J Am Chem Soc, 124 (2002) 9648.
38 Geskin V M, Lambert C & Bredas J L, *J Am Chem Soc*,
    125 (2003) 15651.
39 Kleinman D A, *Phys Rev*, 126 (1962) 1977.
40 Adant M, Dupuis L & Bredas L, *Int J Quantum Chem*,
    56 (1995) 497.
41 Bevan J & Boerio-Goates J, Calculations from statistical
    thermodynamics academic press, 2000.
42 Sajan D, Josepha L, Vijayan N & Karabacak M, *Spectrochim
    Acta Part A Mol Biomol Spectrosc*, 81 (2011) 85.
43 Pearson R G, *J Org Chem*, 54 (1989) 1423.
44 Parr R G & Pearson R G, *J Am Chem Soc*, 105 (1983) 7512.
45 Geerlings P, De Proft F & Langenaeker W, *Chem Rev*,
    103 (2003) 1793.
46 Parr R G, Szentpaly L & Liu S, *J Am Chem Soc*, 121 (1999)
    1922.
47 Chattaraj K & Giri S, *J Phys Chem A*, 111 (2007) 11116.
48 Padmanabhan J, Parthasarathi R, Subramaniaan V &
    Chattaraj P K, *J Phys Chem A*, 111 (2007) 1358.